Penetration of Fields Through a Circular Hole in a Wall of Finite Thickness

Robert L. Gluckstern and John A. Diamond

Abstract—**We consider a uniform, static electric field on one side of a plane metallic wall of finite thickness with a circular hole. The field induces a charge distribution on the metallic surface which behaves, at large distances from the hole, as a dipole moment, with different values for the polarizability on the *inside* (same side as the driving field) and *outside* surfaces of the hole. We have derived two integral equations for the potential in the hole and constructed variational forms for the "symmetric" and "asymmetric" polarizabilities. Trial functions with adjustable parameters lead to accurate numerical values for the "inside" and "outside" polarizabilities. A similar approach yields corresponding values for the "inside" and "outside" magnetic susceptibilities.**

I. Introduction

THE penetration of fields through a small, arbitrarily shaped hole in the wall of a cavity is generally calculated in the idealized case of a cavity with walls of zero thickness. In an earlier paper [1] we constructed variational expressions for the electric polarizability and magnetic susceptibility of such a hole from integral equations for the potential and field distribution within the hole. Exact expressions for the fields' penetration through circular and elliptical holes had previously been derived by Bethe more than 40 years ago [2], [3].

Interest in the case of finite wall thickness has also existed for more than 20 years.[1] In the present work we confine our attention to a circular hole in a plane wall of *finite* thickness with a uniform electric or magnetic "far field" on one side. By separating the problem into symmetric and asymmetric problems with regard to the wall, we are able once again to derive integral equations for the potential and field distribution within the hole and to construct variational expressions for the "symmetric" and "asymmetric" polarizability and susceptibility. A judicious choice of trial functions enables us to obtain highly accurate numerical results for the polarizability and susceptibility of the circular hole for a wall of finite thickness.

II. Zero Wall Thickness

The electric field near a circular hole in a conducting wall can be separated into two fields, one corresponding to a symmetric (with respect to $z \to -z$) configuration of the potential about the hole and one corresponding to an asymmetric configuration (Fig. 1).

If the conducting wall has zero thickness, then the asymmetric potential will have an electric field which is constant in all space and the potential will be given by (we omit the factor $E_0/2$)

$$\Phi_a = z. \tag{1}$$

The general solution for the symmetric potential is

$$\Phi_s(x,y,z) = |z| + \int_{-\infty}^{\infty}\int_{-\infty}^{\infty} dk\,dl\,a_s(k,l)e^{ikx+ily-\sigma|z|} \tag{2}$$

where

$$\sigma = \sqrt{k^2+l^2} \tag{3}$$

and $a_s(k,l)$ is to be determined. Denoting the potential in the hole by

$$f_s(x,y) = \Phi_s(x,y,0) \tag{4}$$

an inverse Fourier transform at $z=0$ immediately yields

$$a_s(k,l) = \frac{1}{4\pi^2}\iint_{\text{hole}} dx\,dy\,e^{-ikx-ily} f_s(x,y) \tag{5}$$

where the integrand vanishes outside the hole region. We now use the continuity of $\partial\Phi/\partial z$ in the hole to get

$$\int_{-\infty}^{\infty}\int_{-\infty}^{\infty} dk\,dl\,\sigma a_s(k,l)e^{ikx+ily} = 1. \tag{6}$$

Substituting for $a_s(k,l)$ and simplifying notation with

$$\vec{\sigma} = k\hat{i} + l\hat{j} \qquad \vec{r} = x\hat{i} + y\hat{j} \tag{7}$$

we obtain

$$\int d\vec{r}\,' f_s(\vec{r}\,')\hat{K}_s(\vec{r},\vec{r}\,') = 1 \tag{8}$$

where

$$\hat{K}_s(\vec{r},\vec{r}\,') = \frac{1}{4\pi^2}\int d\vec{\sigma}\,\sigma e^{i\vec{\sigma}\cdot(\vec{r}-\vec{r}\,')} = -\frac{1}{2\pi|r-r'|^3}. \tag{9}$$

The solution to (8) is

$$f_s(\vec{r}) = \frac{2}{\pi}\sqrt{a^2-r^2} \tag{10}$$

where a is the radius of the hole [2], [3].

Similarly, for the magnetic problem with an asymptotic field $H_x = H_0$ as $z \to \infty$, we obtain for the symmetric H_z component (omitting the factor $H_0/2$)

$$\int d\vec{r}\,' g_s(\vec{r}\,')K_s(\vec{r},\vec{r}\,') = x \tag{11}$$

Manuscript received March 12, 1990; revised August 21, 1990. This work was supported by the U.S. Department of Energy.

R. L. Gluckstern is with the Physics Department, University of Maryland, College Park, MD 20742.

J. A. Diamond was with the Physics Department, University of Maryland, College Park. He is now with Adroit Systems, Inc., Alexandria, VA 22314.

IEEE Log Number 9041466.

[1] A bibliography for apertures in a thick screen was given in 1978 by Butler *et al.* [4]. See also [5] for an infinitely thick wall and [6] and [7] for more recent work with narrow slot apertures with depth.

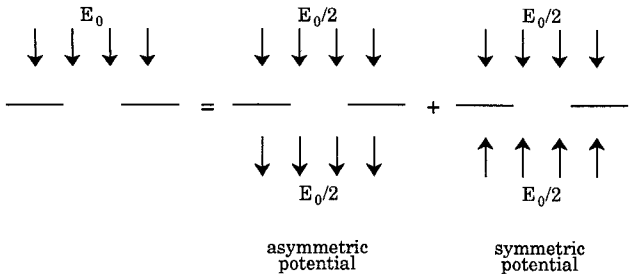

Fig. 1. Separation of electric field into a symmetric and an asymmetric component (zero wall thickness).

with

$$K_s(\vec{r},\vec{r}') = \frac{1}{4\pi^2}\int \frac{d\vec{\sigma}}{\sigma} e^{i\vec{\sigma}\cdot(\vec{r}-\vec{r}')} = \frac{1}{2\pi|r-r'|}. \quad (12)$$

Here $g_s(\vec{r}) = H_{z,s}(x,y,0)$ vanishes outside the hole region. The solution for the magnetic potential in the hole is [2], [3]

$$g_s(\vec{r}) = \frac{4}{\pi}\frac{x}{\sqrt{a^2-r^2}}. \quad (13)$$

As before, the asymmetric H_z component corresponds to a uniform H_x in all of space.

From the potentials in the hole, the polarizability and susceptibility can be determined. An asymptotically uniform electric field $\vec{E}_0$ on one side of a thin wall with a circular hole induces a dipole moment in the wall given by

$$\vec{p} = \chi\epsilon\vec{E}_0, \qquad \chi = \int d\vec{r} f_s(\vec{r}) = \frac{4}{3}a^3 \quad (14)$$

where χ is the electric polarizability of the hole. Similarly, for an asymptotically uniform magnetic field $\vec{H}_0$ on one side of the thin wall, the induced magnetic moment is

$$\vec{m} = \overleftrightarrow{\psi}\cdot\vec{H}_0 \qquad \psi_{xx} = \int d\vec{r} x g_s(\vec{r}) = 8a^3/3$$

$$\psi_{yy} = 8a^3/3 \quad (15)$$

where ψ_{xx} and ψ_{yy} are the diagonalized magnetic susceptibilities of the hole.

III. Variational Formulation for Finite Wall Thickness

When we have an electric or magnetic field in the vicinity of a small circular hole of radius a in a conducting wall with finite thickness L, we begin, as in the zero thickness case, with a separation of the problem into symmetric and asymmetric parts. The electric case is shown in Fig. 2.

A. Electric

In the case of the symmetric potential depicted in Fig. 2, the potential in the region $|z| \geq L/2$ can be written as

$$\Phi_s(\vec{r},z) = |z| - L/2 + \int d\vec{\sigma} a_s(\vec{\sigma}) e^{i\vec{\sigma}\cdot\vec{r} - \sigma(|z|-L/2)}. \quad (16)$$

The first term in (16) corresponds to the asymptotic field $E_z = \pm 1$ as $|z| \to \infty$, while the second term, which corresponds to the potential from the induced charges on the metal surface, satisfies Laplace's equation and vanishes as $|z| \to \infty$.

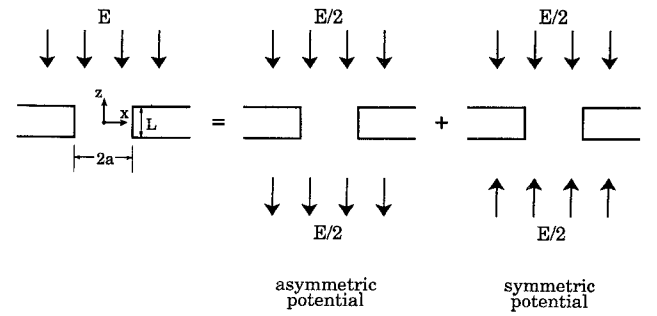

Fig. 2. An electric field incident on a circular hole of radius a in a wall of finite thickness L is split into two components: one with an asymmetric potential and one with a symmetric potential about the midpoint of the wall.

Defining the potential at $z = L/2$ to be $f_s(\vec{r})$, an inverse Fourier transform leads to

$$a_s(\vec{\sigma}) = \frac{1}{4\pi^2}\int_{\text{hole}} d\vec{r} e^{-i\vec{\sigma}\cdot\vec{r}} f_s(\vec{r}). \quad (17)$$

In the region $-L/2 \leq z \leq L/2$, we expand Φ_s in terms of a set of normalized functions $\phi_n(x,y)$ which satisfy the boundary condition that $\vec{E}$ is purely radial at $r = a$. The function $\phi_n(\vec{r})$ is just the normalized $J_0(p_n r/a)$, where p_n is the nth zero of $J_0(p)$. Expanding in that region gives us

$$\Phi_s(\vec{r},z) = \sum_n b_n \phi_n(\vec{r}) \cosh(\gamma_n z), \qquad |z| \leq L/2 \quad (18)$$

where

$$\gamma_n = p_n/a. \quad (19)$$

We choose $\cosh(\gamma_n z)$ since we have a symmetric potential.

Matching the potential at $z = L/2$ gives us

$$\Phi_s(\vec{r}, L/2) = f_s(\vec{r}) = \sum_n b_n \phi_n(\vec{r}) \cosh(\gamma_n L/2) \quad (20)$$

from which we obtain the coefficients b_n:

$$b_n = \frac{1}{\cosh(\gamma_n L/2)} \int d\vec{r} f_s(\vec{r}) \phi_n(\vec{r}) \quad (21)$$

where the integrand vanishes outside the hole region. From the continuity of $\partial\Phi_s/\partial z$ at $z = L/2$, we obtain the relation

$$\sum_n \gamma_n b_n \phi_n(\vec{r}) \sinh(\gamma_n L/2) = 1 - \int d\vec{\sigma}\sigma a_s(\vec{\sigma}) e^{i\vec{\sigma}\cdot\vec{r}}. \quad (22)$$

Using (17) and (21), we obtain the integral equation

$$\int d\vec{r}' f_s(\vec{r}') \hat{K}_s(\vec{r},\vec{r}') = 1 \quad (23)$$

with the kernel $\hat{K}_s$ given by

$$\hat{K}_s(\vec{r},\vec{r}') = \frac{1}{4\pi^2}\int d\vec{\sigma}\sigma e^{i\vec{\sigma}\cdot(\vec{r}-\vec{r}')} + \sum_{n=1}^{\infty} \gamma_n \tanh(\gamma_n L/2) \phi_n(\vec{r}) \phi_n(\vec{r}'). \quad (24)$$

For the asymmetric case, $\cosh(\gamma_n z)$ in (18) is replaced by $\sinh(\gamma_n z)$, resulting in an asymmetric kernel which differs from the symmetric kernel by having $\coth(\gamma_n L/2)$ instead of $\tanh(\gamma_n L/2)$ in (24). In this case the potential in the hole at $z = L/2$ is denoted by $f_a(\vec{r})$.

If we define

$$\chi_s = \int d\vec{r} f_s(\vec{r}) \tag{25}$$

we can write the following variational form for χ_s:

$$\chi_s^{-1} = \frac{\int d\vec{r} \int d\vec{r}' f_s(\vec{r}) f_s(\vec{r}') \hat{K}_s(\vec{r}, \vec{r}')}{\left[\int d\vec{r} f_s(\vec{r})\right]^2}. \tag{26}$$

We use as a trial function the series

$$f_s(\vec{r}) = \sum_m (m+1) c_m \left(1 - \frac{r^2}{a^2}\right)^m \tag{27}$$

where c_m are coefficients which will be chosen to minimize χ_s^{-1} in (26). For a thin wall, the behavior of the potential will be similar to that for $L = 0$ given by (10). In this case we therefore let m take on the values

$$m = \frac{1}{2}, \frac{3}{2}, \frac{5}{2}, \cdots \tag{28}$$

making $f_s(\vec{r})$ in (27) correspond to the zero thickness result multiplied by a Taylor series in powers of $1 - r^2/a^2$.

For a thick wall, the potential at a 90° corner varies as $R^{2/3}$, where R is the distance from the vertex. In this case the leading term with the appropriate behavior at the vertices is

$$\left(1 - \frac{r^2}{a^2}\right)^{2/3}$$

and we therefore let m take on the values

$$m = \frac{2}{3}, \frac{5}{3}, \frac{8}{3}, \cdots \tag{29}$$

for which $f_s(\vec{r})$ has the correct singular behavior at $r^2 = a^2$. In fact, we use both sets of values for m in our numerical work and find reasonable agreement between the two results. But the sequence in (29) leads to the most rapid convergence for all $L/a \neq 0$ since it corresponds to the trial function with the correct behavior near $r^2 = a^2$.

The variational equation, after algebraic manipulation, becomes

$$\frac{\pi a^3}{2} \chi_s^{-1} = \frac{\sum_l \sum_m c_l c_m (\hat{K}_s)_{lm}}{\left(\sum_l c_l\right)^2} \tag{30}$$

where $(\hat{K}_s)_{lm}$ is given by

$$(\hat{K}_s)_{lm} = \frac{\Gamma(l+2)\Gamma(m+2)\Gamma(l+m)\Gamma(3/2)}{\Gamma(l+1/2)\Gamma(m+1/2)\Gamma(l+m+3/2)} + \Gamma(l+2)\Gamma(m+2) \cdot \sum_{n=1}^{\infty} \frac{J_{l+1}(p_n) J_{m+1}(p_n) \tanh(p_n L/2a)}{J_1^2(p_n)(p_n/2)^{l+m+1}}. \tag{31}$$

In evaluating $\int d\vec{r} \int d\vec{r}' f_s(\vec{r}) f_s(\vec{r}') \hat{K}_s(\vec{r}, \vec{r}')$, we have used

$$\int d\vec{r} \left(1 - \frac{r^2}{a^2}\right)^m e^{i\sigma \vec{r}\cdot\vec{r}'} = 2\pi \int_0^a r dr \left(1 - \frac{r^2}{a^2}\right)^m J_0(\sigma r) = \pi a^2 m! \left(\frac{2}{\sigma a}\right)^{m+1} J_{m+1}(\sigma a) \tag{32}$$

where the last form is obtained by expanding $J_0(\sigma r)$ in powers of (σr) [1]. We have also used [8]

$$\int_0^\infty d\sigma \frac{J_\mu(\sigma a) J_\nu(\sigma a)}{\sigma^\lambda} = \frac{\left(\frac{a}{2}\right)^{\lambda-1} \Gamma(\lambda) \Gamma\left(\frac{\mu+\nu-\lambda+1}{2}\right)}{2\Gamma\left(\frac{\lambda+\nu-\mu+1}{2}\right)\Gamma\left(\frac{\lambda+\nu+\mu+1}{2}\right)\Gamma\left(\frac{\lambda+\mu-\nu+1}{2}\right)}. \tag{33}$$

From (30) and the variational principle, we want to minimize $\Sigma_l \Sigma_m c_l c_m (\hat{K}_s)_{lm}$ subject to the constraint that $\Sigma_l c_l =$ constant. Using λ as a Lagrange multiplier, the minimization of the function

$$Q = \sum_l \sum_m c_l c_m (\hat{K}_s)_{lm} - 2\lambda \sum_l c_l \tag{34}$$

occurs when

$$c_l = \lambda \sum_m (\hat{K}_s^{-1})_{lm} \tag{35}$$

where $\hat{K}_s^{-1}$ is the inverse of the matrix $\hat{K}_s$. Equation (30) then relates χ_s to the sum of all the elements of $\hat{K}_s^{-1}$ by

$$\frac{2}{\pi a^3} \chi_s = \sum_l \sum_m (\hat{K}_s^{-1})_{lm}. \tag{36}$$

The analysis for the asymmetric potential is nearly identical, the only difference being the replacement of $\tanh(p_n L/2a)$ in (31) by $\coth(p_n L/2a)$. The variational result for χ_a is therefore given by

$$\frac{2}{\pi a^3} \chi_a = \sum_l \sum_m (\hat{K}_a^{-1})_{lm}. \tag{37}$$

One can now express the results in terms of an induced electric dipole moment. The polarizability related to the induced dipole moment seen *inside* the cavity (on the side where there is a driving field) is

$$\chi_{\text{in}} = \int d\vec{r} [f_s(\vec{r}) + f_a(\vec{r})] = \chi_s + \chi_a \tag{38}$$

while the polarizability related to the induced dipole moment seen *outside* the cavity is

$$\chi_{\text{out}} = \int d\vec{r} [f_s(\vec{r}) - f_a(\vec{r})] = \chi_s - \chi_a. \tag{39}$$

B. Magnetic

As in the electric case, a magnetic field incident on a conducting surface with a circular hole can be divided into a symmetric and an asymmetric mode, as shown in Fig. 3. In

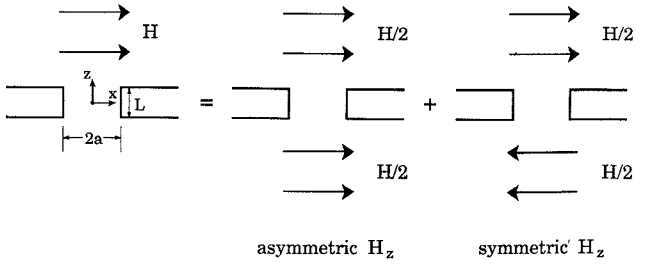

Fig. 3. Separation of magnetic field into symmetric and asymmetric components.

the region $z \geq L/2$, a scalar potential which satisfies the magnetic boundary conditions is given by

$$\Psi(x,y,z) = x + \int d\vec{\sigma}\, b(\vec{\sigma}) e^{i\vec{\sigma}\cdot\vec{r} - \sigma(z-L/2)}, \qquad z \geq L/2. \tag{40}$$

Differentiating gives us the magnetic field:

$$H_z = \frac{\partial \Phi}{\partial z} = -\int d\vec{\sigma}\, b(\vec{\sigma}) \sigma e^{i\vec{\sigma}\cdot\vec{r} - \sigma(z-L/2)}. \tag{41}$$

Defining

$$H_z(x,y,L/2) = g(\vec{r}) \tag{42}$$

allows us to express $b(\vec{\sigma})$ via an inverse Fourier transform as

$$\sigma b(\vec{\sigma}) = -\frac{1}{4\pi^2}\int d\vec{r}\, g(\vec{r}) e^{-i\vec{\sigma}\cdot\vec{r}}. \tag{43}$$

For the symmetric H_z case, we can write the potential in the region $-L/2 \leq z \leq L/2$ as

$$\Psi_s = \sum_n a_n \sinh(\gamma_n z)\psi_n(\vec{r}), \qquad |z| \leq L/2 \tag{44}$$

where the normalized functions $\psi_n(\vec{r})$ satisfy the magnetic boundary condition

$$\left.\frac{\partial \psi_n}{\partial r}\right|_{r=a} = 0. \tag{45}$$

Here, $\psi_n(\vec{r})$ is just the normalized $J_1(q_n r/a)\cos\theta$, where $q_n = \gamma_n a$ is the nth zero of $J_1'(q)$.

We can express the coefficients a_n in (44) in terms of $g_s(\vec{r})$ by recognizing the fact that the $\psi_n(\vec{r})$ form a complete set in the interval $0 \leq r \leq a$. This yields

$$a_n = \frac{1}{\gamma_n \cosh(\gamma_n L/2)} \int d\vec{r} g_s(\vec{r})\psi_n(\vec{r}). \tag{46}$$

Then, using the continuity of Ψ_s at $z = L/2$, we equate (44) and (40) using (43) and (46) to obtain

$$\int d\vec{r}'\, g_s(\vec{r}')\tilde{K}_s(\vec{r},\vec{r}') = x \tag{47}$$

where

$$\tilde{K}_s(\vec{r},\vec{r}') = \frac{1}{4\pi^2}\int \frac{d\vec{\sigma}}{\sigma} e^{i\vec{\sigma}\cdot(\vec{r}-\vec{r}')} + \sum_n \frac{\tanh(\gamma_n L/2)}{\gamma_n}\psi_n(\vec{r})\psi_n(\vec{r}'). \tag{48}$$

Defining

$$\psi_s = \int d\vec{r} x g_s(\vec{r}) \tag{49}$$

allows us to express the magnetic susceptibility in the variational form

$$\psi_s^{-1} = \frac{\int d\vec{r}\int d\vec{r}'\, g_s(\vec{r}) g_s(\vec{r}')\tilde{K}_s(\vec{r},\vec{r}')}{\left(\int d\vec{r} x g_s(\vec{r})\right)^2}. \tag{50}$$

We use as our trial function

$$g_s(\vec{r}) = r\cos\theta \sum_m m(m+1)c_m\left(1-\frac{r^2}{a^2}\right)^{m-1} \tag{51}$$

where the factor $r\cos\theta$ is required by the presence of $x = r\cos\theta$ on the right side of (47). As in the electric case, the limiting forms suggest rapid convergence of the series by using (28) for a thin wall and (29) for a thick wall.

Using relations similar to those in the electric case, we finally obtain

$$\left(\tilde{K}_s\right)_{lm} = \frac{\Gamma(l+2)\Gamma(m+2)\Gamma(l+m)\Gamma(3/2)}{2\Gamma(l+1/2)\Gamma(m+1/2)\Gamma(l+m+3/2)} + \Gamma(l+2)\Gamma(m+2) \cdot \sum_{n=1}^{\infty} \frac{J_{l+1}(q_n)J_{m+1}(q_n)\tanh(q_n L/2a)}{J_1^2(q_n)(q_n - 1/q_n)(q_n/2)^{l+m}} \tag{52}$$

where the variational form relates ψ_s to the kernel by

$$\frac{2}{\pi a^3}\psi_s = \sum_l \sum_m \left(\tilde{K}_s^{-1}\right)_{lm}. \tag{53}$$

For the asymmetric case, $\sinh(\gamma_n z)$ is replaced by $\cosh(\gamma_n z)$ in (44), resulting in $\tanh(q_n L/2a)$ being replaced by $\coth(q_n L/2a)$ in (52). Defining

$$\frac{2}{\pi a^3}\psi_a = \sum_l \sum_m \left(\tilde{K}_s^{-1}\right)_{lm} \tag{54}$$

the susceptibility seen within the cavity is given by

$$\psi_{\text{in}} = \psi_s + \psi_a \tag{55}$$

while the susceptibility seen outside the cavity is given by

$$\psi_{\text{out}} = \psi_s - \psi_a \tag{56}$$

by analogy with (38) and (39).

IV. Numerical Results

By using the variational method, we were able to obtain values for the polarizability and susceptibility accurate to five decimal places.[2] Table I lists $3\chi/8a^3$ and $3\psi/8a^3$ for various thickness-to-radius (L/a) ratios. The polarizabilities and susceptibilities seen both inside and outside the cavity are given. In Fig. 4 we show $3\chi_{\text{in}}/8a^3$ and $3\psi_{\text{in}}/8a^3$ as functions of L/a. Fig. 5 shows the dependence of $\ln(3\chi_{\text{out}}/8a^3)$ and $\ln(3\psi_{\text{out}}/8a^3)$ on L/a, and is in excellent agreement with results quoted by McDonald [5].

[2] We found that the series for $3\chi/8a$ and $3\psi/8a$ starting with $m = 2/3$ converged to five decimal palaces for $L/a \geq 0.001$ and therefore used only this sequence for the results in Table I. We cut off the sums over n in (31) and (32) when $p_n L/2a \simeq 10$ and $q_n L/2a \simeq 10$ and obtained optimum convergence with eight terms in the series for l or m.

TABLE I

	$\frac{3}{8a^3}(\chi_s+\chi_a)$	$\frac{3}{8a^3}(\psi_s+\psi_a)$	$\frac{3}{8a^3}(\chi_s-\chi_a)$	$\frac{3}{8a^3}(\psi_s-\psi_a)$
0	0.50000	1.00000	0.50000	1.00000
0.001	0.49849	0.99640	0.49732	0.99522
0.003	0.49629	0.99084	0.49279	0.98732
0.01	0.49053	0.97537	0.47904	0.96373
0.03	0.47951	0.94284	0.44636	0.90863
0.1	0.45883	0.87143	0.36017	0.76404
0.3	0.43826	0.77829	0.21014	0.50124
1.0	0.42950	0.71467	0.03740	0.13340
3.0	0.42923	0.70987	0.00030	0.00335
10.0	0.42923	0.70987	0.00000	0.00000
∞	0.42923	0.70987	0.00000	0.00000

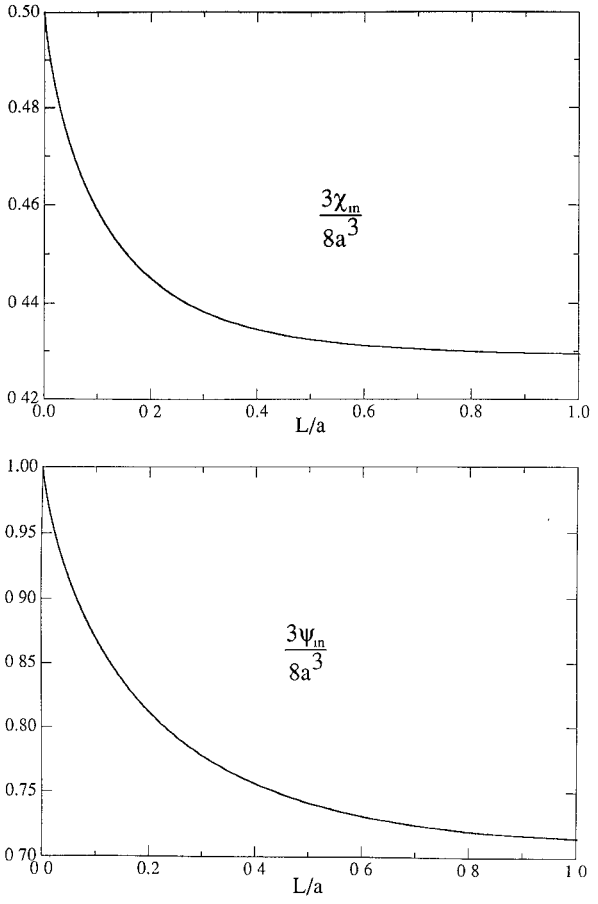

Fig. 4. "Inside" polarizability and susceptibility as a function of wall thickness.

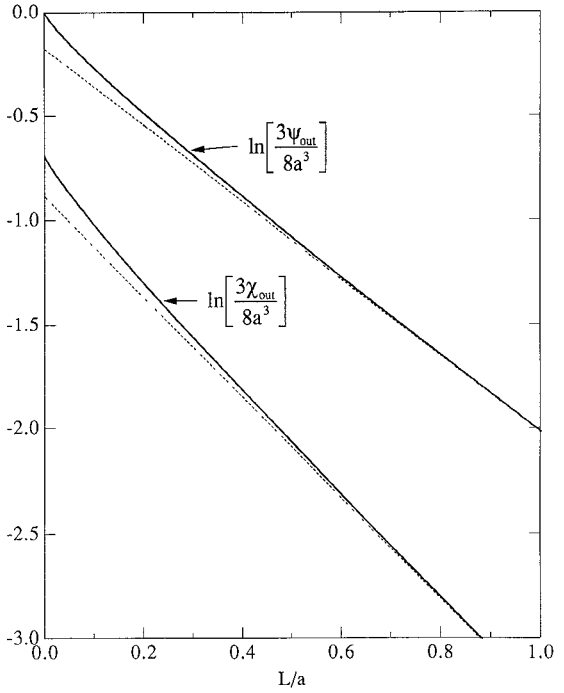

Fig. 5. "Outside" polarizability and susceptibility as a function of wall thickness. The dashed lines are the asymptotic limits for thick walls.

As $L/a \to 0$, we recover the zero thickness results:

$$\chi_{out} = \chi_{in} \to 4a^3/3 \qquad \psi_{out} = \psi_{in} \to 8a^3/3. \quad (57)$$

As $L/a \to \infty$, the logarithmic graphs become linear with slopes -2.405 and -1.841, respectively, for the polarizability and susceptibility. These asymptotic limits are shown as dashed lines in Fig. 5 and are given by

$$\ln\left(3\chi_{out}/8a^3\right) \to -2.405(L/a) - 0.886 \quad (58)$$

$$\ln\left(3\psi_{out}/8a^3\right) \to -1.841(L/a) - 0.716. \quad (59)$$

The fact that the slopes equal the first zeros of $J_0(p)$ and $J_1'(q)$ reflects the dominance of the lowest modes, i.e., the modes with the smallest exponential drop-off along the z axis, for thick walls. The numerical constant in (59) agrees exactly with that of Latham and Lee [5] for magnetic penetration into a semi-infinite pipe.

For small L/a, one can use the stationary forms in (26) and (50) to show that

$$\frac{3\chi_s}{8a^3} \cong \frac{1}{2} - \frac{3L}{4\pi a}\left(\ln\frac{a}{L} + A\right) \quad (60)$$

$$\frac{3\psi_s}{8a^3} \cong 1 - \frac{3L}{2\pi a}\left(\ln\frac{a}{L} + A'\right) \quad (61)$$

$$\frac{3\chi_a}{8a^3} \cong \frac{3\psi_a}{8a^3} \cong \frac{3\pi L}{16a} \quad (62)$$

where the numerical values[3] $A \cong 1.88 \pm 0.02$ and $A' \cong 1.88 \pm 0.02$ are obtained by using the values in Table I for $L/a \leqslant 0.03$. The infinite slope at $L/a = 0$ indicated by (60) and

[3]The numerical results indicate that $A = A'$. We cannot prove this assertion.

(61) accounts for the curvature seen in Figs. 4 and 5 near $L/a = 0$.

V. Summary

We have derived integral equations for the potential and field distribution within a circular hole in a plane conducting wall of finite thickness induced by uniform "far fields." Variational expressions are then obtained for the polarizability and susceptibility of the hole, from which one can obtain the electric and magnetic dipole moments induced on the inside (far field) and outside (no far field) boundaries of the hole. A choice of trial functions with adjustable parameters which takes into account the expected potential and field behavior near the hole corners and edges leads to numerical values accurate to approximately 10 p.p.m.

Acknowledgment

One of the authors (RLG) would like to thank Dr. A. C. Melissinos for calling his attention to the work of McDonald [9] and to some experimental measurements consistent with McDonald's predictions [10].

References

[1] R. L. Gluckstern, R. Li, and R. K. Cooper, "Electric polarizability and magnetic susceptibility of small holes in a thin screen," *IEEE Trans. Microwave Theory Tech.*, vol. 38, pp. 186–192, Feb. 1990. Correction: vol. 38, pp. 1529–1530, Oct. 1990.
[2] H. A. Bethe, *Phys. Rev.*, vol. 66, p. 163, 1944.
[3] R. E. Collin, *Field Theory of Guided Waves*. New York: McGraw-Hill, 1960.
[4] C. M. Butler, Y. Rahmat-Samii, and R. Mittra, "Electromagnetic penetration through apertures in conducting surfaces," *IEEE Trans. Antennas Propagat.*, vol. AP-26, p. 82, Jan. 1978.
[5] R. W. Latham and K. S. H. Lee, "Magnetic field leakage into a semi-infinite pipe," *Can. J. Phys.*, vol. 46, p. 1455, 1968.
[6] L. K. Warne and K. C. Chen, "Relation between equivalent antenna radius and transverse line dipole moments of a narrow slot aperture having depth," *IEEE Trans. Electromagn. Compat.*, vol. 30, p. 364, Aug. 1988.
[7] ___, "Equivalent antenna radius for narrow slot apertures having depth," *IEEE Trans. Antennas Propagat.*, vol. 37, p. 824, July 1989.
[8] G. N. Watson, *Theory of Bessel Functions*. New York: Macmillan, 1945, p. 403.
[9] N. A. McDonald, "Electrical and magnetic coupling through small apertures in shield walls of any thickness," *IEEE Trans. Microwave Theory Tech.*, vol. MTT-20, p. 689, Oct. 1972.
[10] C. E. Reece, P. J. Reiner, and A. C. Melissinos, "Parametric converters for detections of small displacements," *Nucl. Instrum. Methods*, vol. A245, p. 299, 1986.

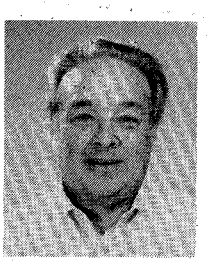

Robert L. Gluckstern received the B.E.E. degree from the City College of the City University of New York in 1944 and the Ph.D. degree from the Massachusetts Institute of Technology in 1948.

After postdoctoral years at the University of California at Berkeley and at Cornell University, he served on the physics faculties of Yale University (1950–1964) and the University of Massachusetts at Amherst (1964–1975). He has been Professor of Physics at the University of Maryland since 1975, with research interests in the theory of particle accelerators.

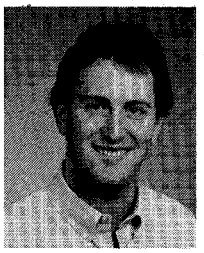

John A. Diamond received the B.S. degrees in physics and computer science from Duke University in 1988. He received the M.S. degree in physics from the University of Maryland in 1990.

He is now with Adroit Systems, Inc., Alexandria, VA.